HIGHER-ORDER BLIND SIGNAL FEATURE SEPARATION: AN ENABLING TECHNOLOGY FOR BATTLEFIELD AWARENESS

Wei Su* and John A. Kosinski
U.S. Army CERDEC, Ft Monmouth, NJ 07703

ABSTRACT

Higher-order transform blind signal feature classification is discussed for separating bar-shaped, circular, squared, circular-squared, and offset-diamonded constellation patterns of digital linear signals. This technique is used for automatic modulation classification of unknown signals. The higher-order transform technique is powerful in distinguishing the geometrical patterns of the signal constellations and can be used to sort a large amount of modulation schemes into several pattern groups with smaller amount of modulation schemes so a fine modulation classification can be performed more effectively and reliably on each pattern group. Robustness of higher-order cumulants is discussed to show that the constellation pattern separation is less sensitive to variations in signal-to-noise ratio.

1. INTRODUCTION

Blind signal separation (BSS) is a critical technology for battlefield situation awareness based upon the tracking of RF transmissions from friendly, hostile, and non-combatant emitters. Within BSS, automatic modulation feature separation and recognition is a key step in classifying signals without prior knowledge of the emitters. With the emergence of software-defined radios and cognitive radios, BSS becomes an attractive research topic in commercial applications. The concept is to exploit the radio transmission environment and choose the best modulation scheme to maximize the channel capacity and minimize interference in real time. In cognitive radios, the signal data can be transmitted frame by frame and the modulation scheme in each data frame can be determined depending upon the channel quality to insure the adaptive modulation scheme maintains the BER below a certain threshold to ensure the QoS in data transmission. Recently, many research results have been published (Su et al., 2002a, 2006) on migrating military BSS to commercial applications in selecting the modulation schemes automatically without the redundant pilot symbols. A common practice is to embed an automated modulation estimator into the receiver of a SDR as shown in Figure 1. The modulation estimator works in parallel with a programmable demodulator in the receiver. A change in the modulation scheme of the transmitter in each data frame will be detected and the demodulator will be cued to change the demodulation scheme accordingly. The modulation estimator classifies modulation schemes by comparing the unknown signal to known templates. The reliability of the estimation largely depends on the crowdedness of the signal space or the size of the template library. The higher-order transform (HOT) is a popular technique adopted to separate unknown signals. HOT may include power-law (DeSimio and Glenn, 1988), moments, cumulants (Swami and Sadler, 2000), and cyclic cumulants (Spooner, 2001; Dobre et al., 2003) approaches which can be used to recognize modulation types such as PSK and squared-QAM. The PSK constellations have circular amplitudes with evenly distributed phases, while the squared-QAM constellations have square amplitudes and dominant phases (at $\pm 45^{o}$ and $\pm 135^{o}$). Such features can be extracted using HOT approaches. Our work applies HOT techniques to a larger variety of signals by including circular-squared-QAM (CSQ) described by MIL-STD-188 110B (DoD Interface Standard, 2000). The CSQ constellations have higher-power unevenly-phased circular amplitudes together with lower-power squares and are relatively featureless to many constellation recognition methods. Thus, a constellation pattern separation technique is developed to sort the unknown signals to five geometrical groups: bar, circle, square, offset-diamond, and circular-square with no prior knowledge of the modulation schemes, so that fine modulation recognition methods can be applied to each geometrical group with much less crowded signal space.

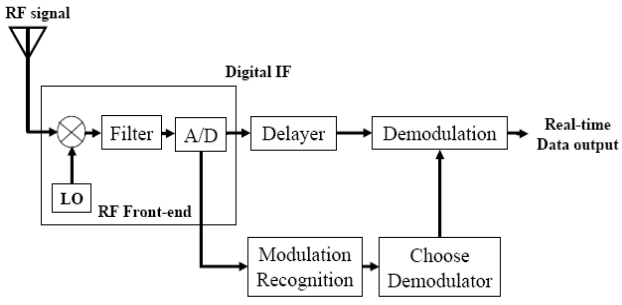

Figure 1. Modulation classification for SDR

Report Documentation Page

Form Approved
OMB No. 0704-0188

1. REPORT DATE	2. REPORT TYPE	3. DATES COVERED
01 NOV 2006	**N/A**	**-**

4. TITLE AND SUBTITLE	5a. CONTRACT NUMBER
Higher-Order Blind Signal Feature Separation: An Enabling Technology For Battlefield Awareness	5b. GRANT NUMBER
	5c. PROGRAM ELEMENT NUMBER
6. AUTHOR(S)	5d. PROJECT NUMBER
	5e. TASK NUMBER
	5f. WORK UNIT NUMBER
7. PERFORMING ORGANIZATION NAME(S) AND ADDRESS(ES) **U.S. Army CERDEC, Ft Monmouth, NJ 07703CA 93106, U.S.A.**	8. PERFORMING ORGANIZATION REPORT NUMBER
9. SPONSORING/MONITORING AGENCY NAME(S) AND ADDRESS(ES)	10. SPONSOR/MONITOR'S ACRONYM(S)
	11. SPONSOR/MONITOR'S REPORT NUMBER(S)

12. DISTRIBUTION/AVAILABILITY STATEMENT
Approved for public release, distribution unlimited

13. SUPPLEMENTARY NOTES
See also ADM002075., The original document contains color images.

14. ABSTRACT

15. SUBJECT TERMS

16. SECURITY CLASSIFICATION OF:			17. LIMITATION OF ABSTRACT	18. NUMBER OF PAGES	19a. NAME OF RESPONSIBLE PERSON
a. REPORT	b. ABSTRACT	c. THIS PAGE			
unclassified	**unclassified**	**unclassified**	**UU**	**7**	

Standard Form 298 (Rev. 8-98)
Prescribed by ANSI Std Z39-18

2. HIGHER ORDER TRANSFORM FEATURES

For a linearly modulated signal transmitted through a flat fading AWGN channel, the digitized signal at the communication receiver can be approximately described as:

$$u(k) = a_c e^{j(2\pi f_c nT+\varphi)} \sum_{n=1}^{N} a_n g_T(\frac{k}{l} - n)T + w_n \qquad (1)$$

where N is a positive integer, w_n is the AWGN, T is the symbol rate, T_s is the sample rate, $l=T/T_s$ is the over-sampling factor, a_n is a complex number represents the *n-th* symbol, $g_T(\cdot)$ is the square-root pulse with unknown shape and roll-off factor, f_c is the residual carrier frequency, a_c is the channel gain, and φ is the combination of carrier and channel phases. In cooperative communication, the receiver down-coverts and matched-filters the RF signal based on prior knowledge of the carrier frequency, symbol rate, bandwidth, pulse shape, etc. The symbol timing, carrier phase, and channel distortion can be estimated by training sequences or hand shaking between transmitter and receiver.

In non-cooperative communication cases such as signal interception and hostile signal detection, the ground truth of the transmitter is unknown and the training sequences are not available. The non-cooperative RF receiver has to estimate the unknown parameters of the transmitted signals, make hypothesis on modulation schemes, and propose the best statistical decisions.

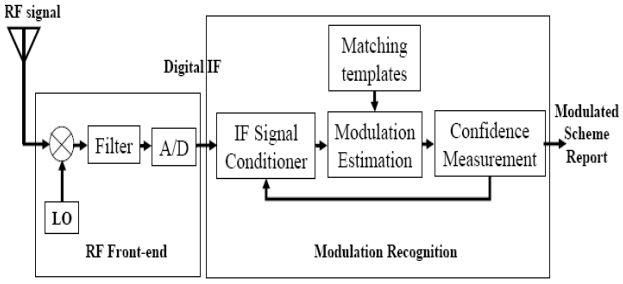

Figure 2. Modulation classification block diagram

As shown in figure 2, the frequency down converter brings the RF signal to near-baseband with a low-pass filter based on the coarse estimation of spectral center frequency and bandwidth. The down converted signal in complex format is over-sampled (for example: 4 samples per symbol) to provide sufficient resolution in signal processing. Then, a snapshot of N digital samples are extracted and buffered for digital signal processing. Before applying HOT techniques for signal separation, the carrier frequency offset and carrier phase offset have to be estimated and removed, the amplitude of the signal has to be normalized, and the channel effects have to be compensated. After IF signal conditioning, the signal can be described by

$$x(k) = \sum_{n=1}^{N} \bar{a}_n g_T(\frac{k}{l} - n)T + \bar{w}_n \qquad (2)$$

where $\bar{w}_n$ is the additive noise assumed to be Gaussian after conditioning, $\bar{a}_n$ is the unknown symbol which belongs to an alphabet set $A_i^j = \{\alpha_1^j, \alpha_2^j, \cdots \alpha_I^j\}$. For modulation classification purposes, we assume there are J number of signals of interest, which are indexed by $j=1, 2, \ldots, J$, and listed in the reference library of the classifier. Signals not listed will be rejected and classified as unknowns. Therefore, the notation α_i^j stands for the i^{th} alphabet of the j^{th} signal, which forms the j^{th} constellation of dimension I. The value of α_i^j is normalized to

$$\sum_{i=1}^{I} \left\| \alpha_i^j \right\| = 1$$

for all j. The signals of interest are described by the following: bar-shaped constellation: PSK2, as shown in figure 3, circular constellations: PSK8 and PSK16 as shown in figure 5, squared constellations: PSK4, QAM16, QAM64, and QAM256, as shown in figure 6, circular-squared constellations: QAM16m, QAM32m, and QAM64m, and crossed constellation: QAM32 as shown in figure 7, and offset-diamonded constellations: V29-8 and V29-16 as shown in figure 8.

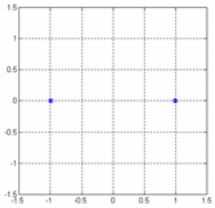

Figure 3. Bar-shaped constellation pattern

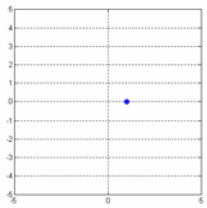

Figure 4. The 4th order bar-shaped constellation pattern

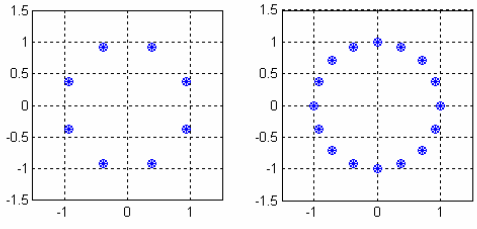

Figure 5. Circular constellation patterns

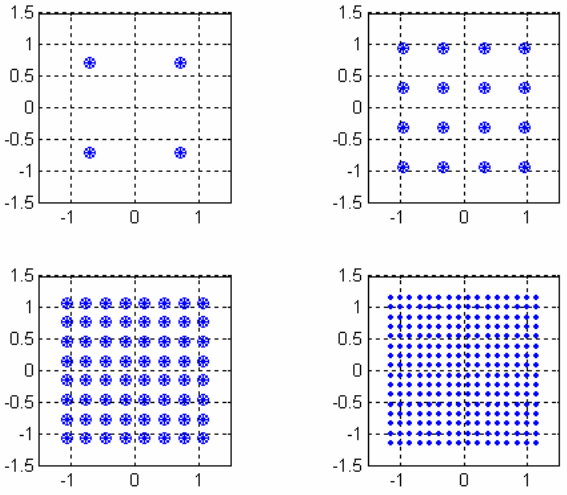

Figure 6. Squared constellation patterns

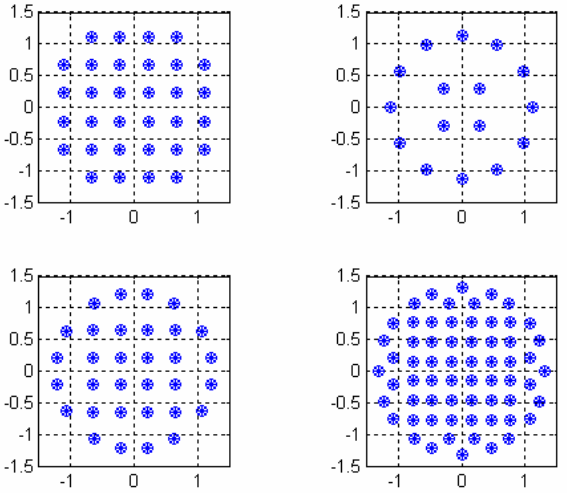

Figure 7. Circular-squared constellation patterns

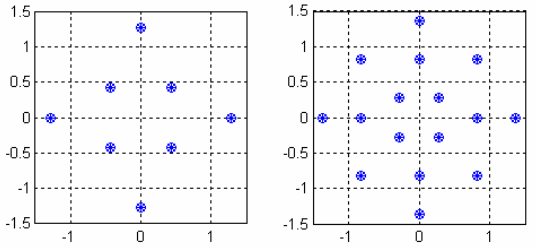

Figure 8. Offset-diamonded constellation patterns

The power-law technique (DeSimio and Glenn, 1988) is used to transform the geometrical patterns of the constellations so that the features of the constellations can be observed. Figure 4, 9-12 demonstrated constellations of the 4th order power-law $(\alpha_i^j)^4$ of the alphabet α_i^j for $i=1, 2, \ldots, I$ and $j=1, 2, \ldots, J$. Examining those 4th order power-law results, we observe that the bar-shaped pattern has a positive real value. The circular patterns are still circular in shape but only contain one fourth of the constellation points, the squared patterns always have negative real values as dominant dots, the circular-squared patterns are all centered at the origin, and the offset-diamonded patterns have a bar-shape pattern which has more weight in the positive real part.

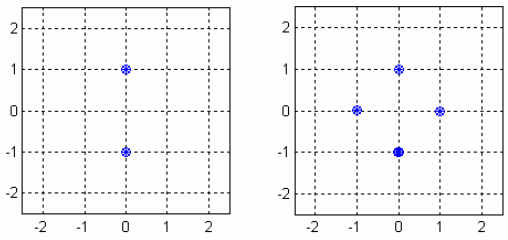

Figure 9. The 4th order power-law circular constellation patterns

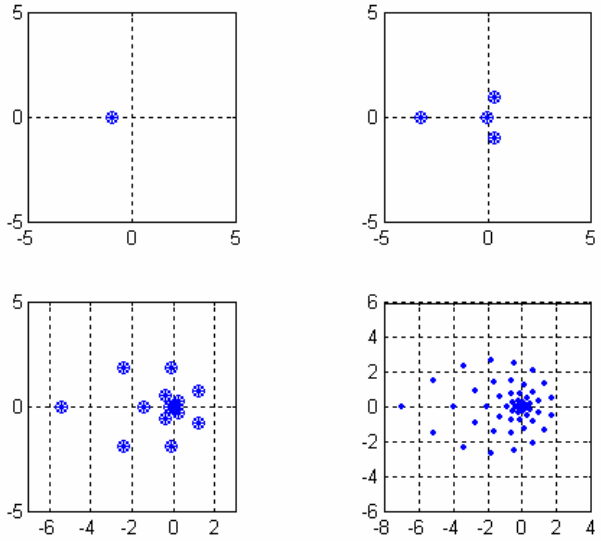

Figure 10. The 4th order power-law squared shaped constellation patterns

If superimposing figures 5-8 to figure 3 and superimposing figure 9-12 to figure 4, as shown in figure 13 and 14, respectively, we notice that the alphabet signal space of the 4th order power-law is much

less crowded and the classification of different alphabet sets (modulation schemes) will be more reliable.

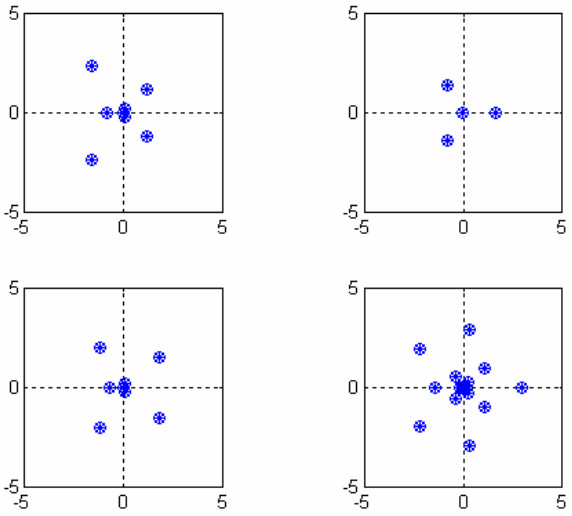

Figure 11. The 4th order power-law circular-squared constellation Patterns

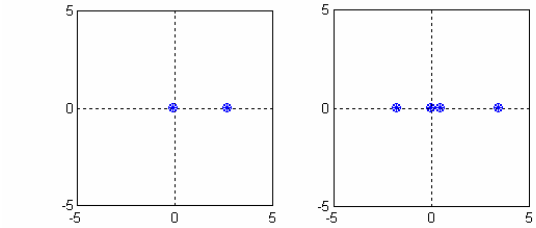

Figure 12 The 4th order power-law offset-diamond shaped constellation Patterns

The high-order features can be measured by calculating complex moments of α_i^j denoted by $m_{pq}^j(\alpha_i^j)$, where p and q are the order and the complex conjugate order of the moment. For example $m_{20}^j(\alpha_i^j)$ of the bar-shaped alphabet constellation pattern, such as PSK2, is nonzero but $m_{20}^j(\alpha_i^j)$ of all other alphabets of constellation patterns are zero. Therefore, bar-shaped constellation patterns can be easily separated from others. Furthermore, the PSK4, PSK8, PSK16 constellations can be identified by using $m_{40}^j(\alpha_i^j)$, $m_{80}^j(\alpha_i^j)$, and $m_{16,0}^j(\alpha_i^j)$, respectively, so that the circular patterns can also be separated from other patterns.

The j^{th} constellation has its own moment $m_{40}^j(\alpha_i^j)$. If a noisy sequence x belongs to $m_{40}^j(\alpha_i^j)$ but the index j is unknown to the user, we can calculate $m_{40}(x)$ and match it to the known moment $m_{40}^j(\alpha_i^j)$, $j=1, 2, \ldots, J$, for the best fit. Unfortunately, the moment operation also amplifies unwanted additive noise and thus is not practical in low SNR applications. The cumulants test (Swami and Sadler, 2000) is a more robust solution by combining various orders of moments with a given formula (Mendel, J., 1991). Unlike moments, the higher-order cumulants are theoretically immunized from the additive Gaussian noise since the higher-order cumulants of a signal plus noise equal the cumulants of the signal plus the cumulants of the noise, and the latter vanishes if it is Gaussian. This makes the higher-order cumulants insensitive to the additive noise even if that noise is colored (Mendel, J., 1991). The cumulant of a random valuable x is denoted by $c_{pq}(x)$, where p and q are the order and the complex conjugate order of the cumulants. Although the cumulants can be computed by the nonlinear combination of moments, the theoretical values are difficult to obtain in practice. For example, the 4th order cumulant $c_{40}(x)$ is computed by

$$c_{40}(x) = m_{40}(x) - 3m_{20}^2(x) = \int x^4 f(x)dx - 3\left(\int x^2 f(x)dx\right)^2, \quad (3)$$

where $f(x)$ is the distribution of the random valuable x. In practice, only a finite number of discrete variables, $x(k)$, are available. The 4th order moment and cumulant of the unknown valuables are then estimated by the time-average of a finite sequence as shown below:

$$m_{40}(x) \approx m_{40} = \sum_{k=1}^{N} x^4(k) \quad (4)$$

$$c_{40}(x) \approx c_{40} = \sum_{k=1}^{N} x^4(k) - 3\left(\sum_{k=1}^{N} x^2(k)\right)^2 \quad (5)$$

In order to investigate the performance change by using the estimated cumulant c_{40}, a computer simulation of the higher order transform of Gaussian noise for both moment m_{40} and cumulant c_{40} are conducted from 0 to 20 dBW. The simulation shows that the value of the 4th order moment m_{40} is decreased at lower SNRs but the value of the 4th order cumulant c_{40} is relatively unchanged. However, when the length of the sample is reduced, the performance of the cumulants becomes degraded. We observe that the 4th order cumulant c_{40} of Gaussian noise with 1,000 samples is less stable than the same noise model with 1,000,000 samples.

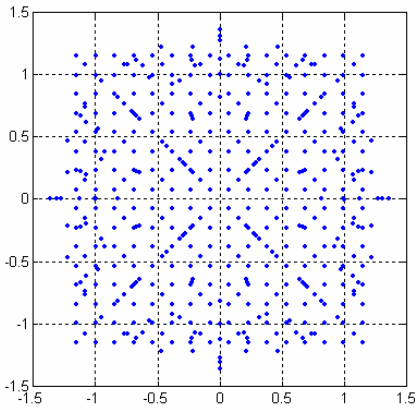

Figure 13. Constellation pattern space

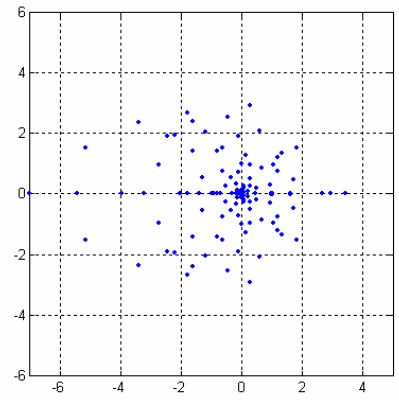

Figure 14. The 4th order power-law constellation pattern space

3. SIGNAL FEATURE SPACE

The objective of HOT approaches is to transform the modulation feather such as amplitude and phase to a more classification friendly domain. To show this, we calculated the cumulants c_{20}, c_{21} c_{40}, c_{41}, c_{42}, c_{60}, c_{61}, c_{62}, c_{63}, c_{80}, c_{81}, c_{82}, c_{83}, and c_{84} for the alphabets of modulation schemes: QPSK; PSK8, PSK16, QAM16, QAM64, QAM32, QAM16m, QAM32m, QAM64m; V29-8, and V29-16; where a modulation type ending with 'm' represents the MIL-STD-188 110B CSQ signals. The HOT feature space can be displayed as a three-dimensional feature space where the *x-axis* denotes modulation schemes, the *y-axis* denotes the types of cumulants, and the *z-axis* shows the values of cumulants. The constellation patterns are distinct for each type and thus can be used to group modulation schemes in the feature space. This can be illustrated as a family of 2D plots for recognition analysis as shown in Figures 15, where the *x-axis* represents the type of cumulants, and the *y-axis* represents the values of cumulants normalized to between 0 and 1. Conventional approaches to recognize modulation schemes would attempt to maximize the likelihood of template matching between the cumulant of unknown noisy data and the cumulant of known alphabets of modulation schemes. This will not work very well since some values of the cumulants, as shown in figure 15, are too close to call.

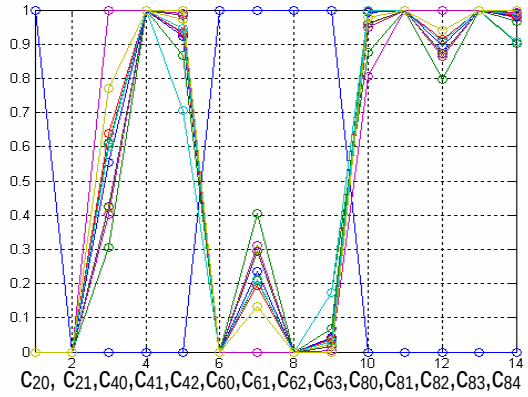

Figure 15. Modulation schemes vs. cumulants

The modulation properties in Figure 15 are not evenly spaced over the feature space, rather, they are better grouped into five sets: {PSK2}, {PSK8, PPSK16}, {QPSK, QAM16, QAM64,}, {QAM32, QAM16m, QAM32m, QAM64m}, and {V29-8, V29-16} as shown in Figure 16-20, respectively.

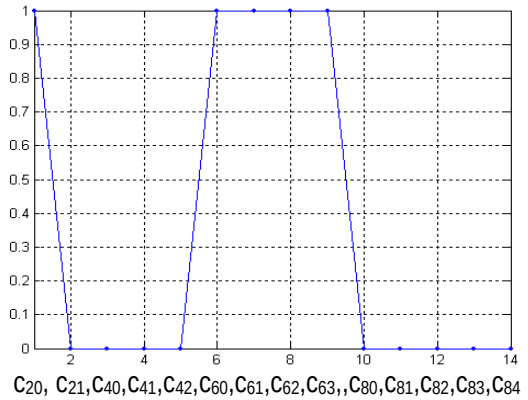

Figure 16. Bar-shaped modulation schemes vs. cumulants

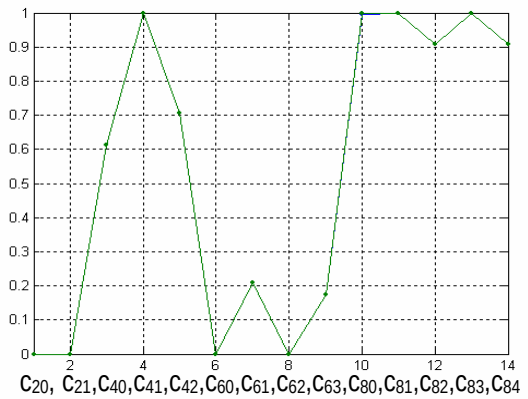

Figure 17. Circular modulation schemes vs. cumulants

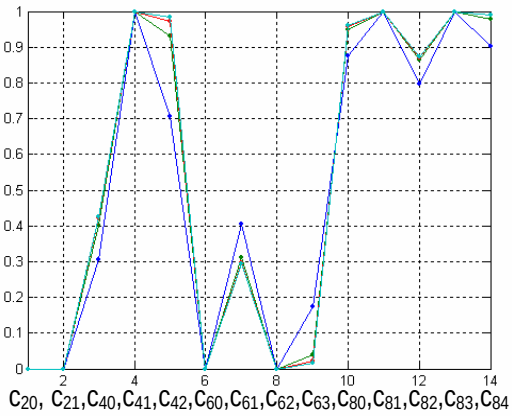

Figure 18. Squared modulation schemes vs. cumulants

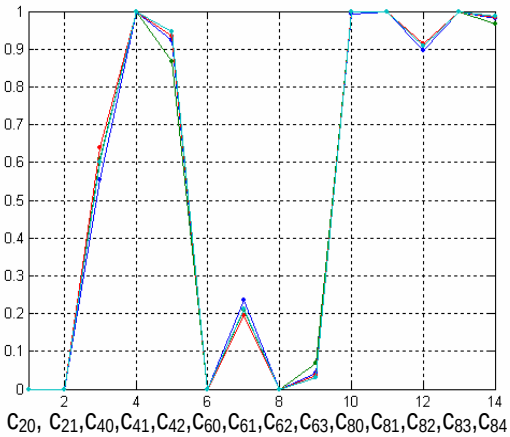

Figure 19. Circular-squared modulation schemes vs. cumulants

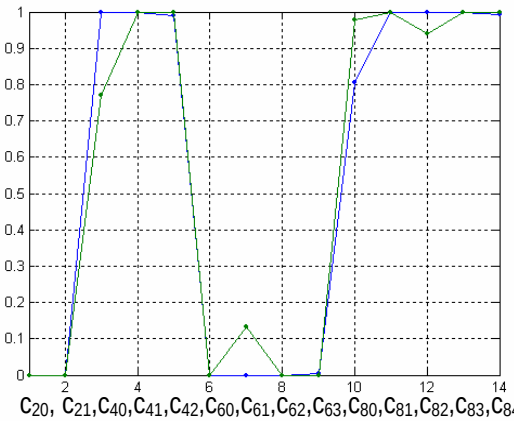

Figure 20. Diamonded modulation schemes vs. cumulants

This leads naturally to a two-stage recognition process. The first stage is a geometrical pattern separation that is critical to dividing signal modulation constellations into 'bar', 'circular,' 'squared', 'circular-squared' and 'offset-diamonded' types. Then it is followed by a fine separation stage that concentrates on the mathematical estimation of HOT features within the group. A brief hierarchical decision tree is shown in Figure 21. We notice that the cumulants can be grouped into five sets C1={c_{40}, c_{61}, c_{82}}, C2={c_{20}, c_{41}, c_{60}, c_{62}, c_{81}, c_{83}}, C3={c_{42}, c_{63}, c_{84}}, and C4={c_{80}} based on the similarity in values. For example, in set C1, the values of c_{40}, c_{61}, and c_{82} are almost equal in values. Therefore if c_{40} is used, c_{61} and c_{82} will be considered as redundant features (which are not significant in providing new information). Since the elements in set C2 are identical for all modulation schemes, it will not contribute in classification. The useful features are narrowed down to c_{40}, c_{42}, and c_{80}. The previous section has discussed how to extract bar-shaped and circular pattern by using moments, the same approach can be extended here by using 4th order cumulants to separate squared, circular-squared, and offset-diamonded patterns.

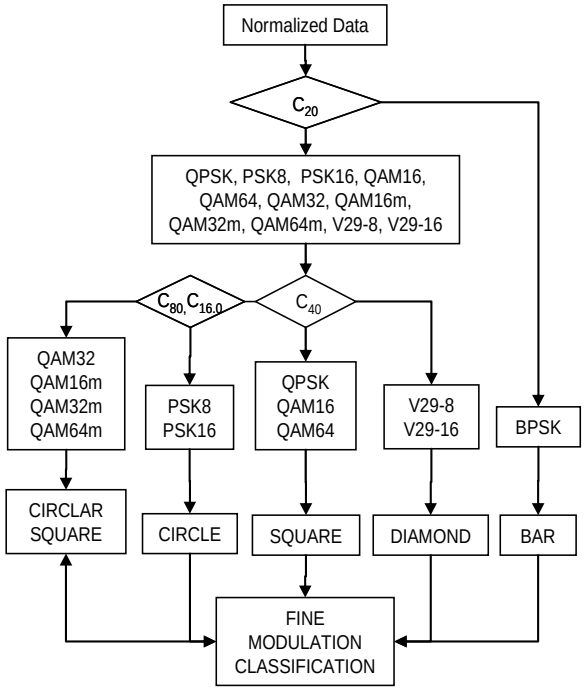

Figure 21. Modulation feature separation decision tree

4. MODULATION PATTERN SEPARATIION

The 4th order cumulant c_{40} reduces the symmetry of the constellation patterns so that constellation points lying on the $\pm 45^{o}$ and $\pm 135^{o}$ lines will be emphasized for separating patterns into three groups: square, circular-square, and offset-diamond. The 4th order cumulant c_{42} captures the amplitude of the constellations. Figure 22 demonstrates values of normalized c_{40} versus SNRs for the signals described by Equation 2 with modulation schemes of QPSK, PSK8, PSK16, QAM16, QAM64, QAM32, QAM16m, QAM32m, QAM64m, V29-8, and

V29-16. A block of 1,000 symbols are used which is over-sampled to 4 samples per symbol. Monte Carlo simulation is conducted. From the top down in figure 25, the first stripe is values of c_{40} versus SNR for 1,000 trials of all squared modulation schemes, the second stripe contains 1,000 trials of all circular modulation schemes, and 1,000 trials of circular-squared modulation schemes, in which the circular types can be further separated by using c_{80} and $c_{16,0}$, as mentioned before, the third and the forth stripes are for 1,000 trials of offset-diamond modulation schemes, where the third one is for V29-16, and the forth one is for V29-8. Notice that those stripes are quite flat, clearly separated, and insensitive to SNRs above 4dB (SNR is defined over the sampling bandwidth). Therefore, the constellation pattern can be reliably separated. Simulation shows that if 4,000 symbols are used, the stripes will be separated even below 4dB SNR. Since the noiseless values of normalized c_{40}s are known for all modulation schemes, least-mean-square error test or many other methods can be used to classify the patterns automatically. Once the patterns are recognized, a fine modulation classification method can be used for further classification. Many fine modulation recognition methods are available and we will not discuss them here. However, it is remarkable that in this new approach, the fine recognition process will apply to a much less crowded signal space to achieve the better performance.

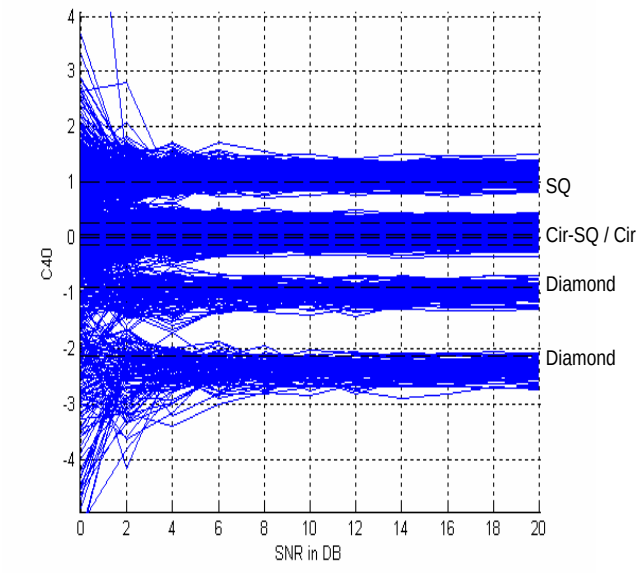

Figure 22. c_{40} vs. SNR

CONCLUSION

The performance of the modulation classification largely depends on the distances in the signal space. The new higher-order signal constellation pattern separation method sorts the signal into several groups so that the signal space in each group is less crowded. Circular-squared constellation pattern can be classified to bar-shaped, circular, squared, and offset-diamond constellation patterns by using the 4th order cumulants. The high-order method may not be effective in identifying a specific modulation scheme but it is very powerful in separating geometrical patterns of constellations for linear modulated digital signals.

REFERENCES

Su, W., Kosinski, J., and Yu, M., 2006: Dual-use of modulation classification techniques for digital communication signals, *Proc. of 2006 IEEE LISAT Conference*, May 2006.

Su, W. and Kosinski, J., 2002: Comparison and modification of automated communication modulation recognition methods, *Proc. of MILCOM'02*, October 2002.

DeSimio, M. and Glenn, E., 1988: Adaptive generation of decision functions for classification of digitally modulated signals, *Proc. Of NAECON'88*, pp. 1010-1014, 1988.

Swami, A. and Sadler, B., 2000: Hierarchical digital modulation classification using cumulants, *IEEE Trans. on Communication*, Vol.48, No.3, March 2000.

Spooner, C., 2001: On the utility of sixth-order cyclic cumulants for RF signal classification, *Proc. ASILOMAR*, 2001, pp. 890-897.

Dobre, O. BarNess, Y., and Su, W., 2003: Higher-order cyclic cumulants for high order digital modulation classification, *Proceedings of IEEE MILCOM 2003*, October 2003.

Mendel, J., 1991: Tutorial on higher-order statistics in signal processing and system theory: theoretical results and some applications, *Proc. of the IEEE*, Vol. 79, No.3, March 1991.

Department of Defense Interface Standard, 2000: *MIL-STD-188-110B*, Interoperability and Performance Standards for Data Modems, Appendix C, pages 93 to 96. April 27, 2000.